

D. Drickey
 Department of Physics
 University of California, Los Angeles
 Los Angeles, California 90024

B. Ecker and S. Putnam
 Physics International Co.,
 San Leandro, California 94577

Further results on the process of coherent acceleration of positive particles by intense electron beams injected into an initially neutral gas are presented. Accelerating fields of the order of one MV per centimeter and proton intensities of 10^{12} protons per pulse have been observed. Proton energy as a function of cathode and gas parameters are also presented. Agreement between the beam current velocity and proton velocity is seen. Acceleration cutoff occurs in a pressure region where beam current velocity increases sharply.

Introduction

In this paper we report on a study of coherent acceleration of protons by intense relativistic electron beams injected into initially neutral gas. As this study is a continuation of previously reported work,¹ we include both new data and, where appropriate for comparison, a compilation of all of the data taken on the Physics International 738 Pulserad electron beam generator. Although many different positive particles have been accelerated (up to 29 MeV N^{+7} ions when nitrogen was used as the gas), the present study concentrated on using hydrogen gas and observing the accelerated protons, since the unique charge to mass ratio of the proton provides a valuable diagnostic tool in understanding the acceleration mechanism.

Apparatus

The vacuum diode of the 738 Pulserad consisted of a flat circular cathode and an aluminized mylar transmission anode. Cathode diameters of 1, 2, and 3 inches and cathode materials of carbon or conductive epoxy were used. Use of a 3/8 inch anode-cathode spacing gave a beam current increasing at 7.5×10^{12} A/sec for 10 nsec, a peak current of more than 100 kA after 35 nsec, and zero current at 100 nsec. Two diode voltages were used, corresponding to peak voltages of 1.0 MV and 750 kV at about $t = 10$ nsec and decreasing to zero volts at 90 nsec. For these differing diode voltages, peak diode currents were virtually the same although details of risetimes and other injected beam parameters were slightly different. We use the nomenclature 1.0 MV and 750 kV to refer to these two beams but caution that these are nominal values only so far as detailed parameters are concerned. The beam was injected into the proton acceleration chamber, a 3 inch diameter copper tube filled with the hydrogen gas at various pressures. Chamber length was 82 cm for the 750 kV beams and 73 cm for the 1.0 MV beams. Transmitted electron beam current wave forms and the position of the beam front versus time were measured using four Rogowski coils recessed in the tube wall at 1, 5, 14.7 and 49.4 cm from the anode. A 1.1 cm diameter tube, 20 cm long, separated the acceleration tube from the low vacuum proton diagnostic region and served as an impedance for differential pumping or, at the higher pressures, was covered with a 2.5 micron mylar foil for the same purpose. Electrons traversing this tube were stripped away from the protons by space charge forces and by a transverse 1 kG field extending 6 inches

along the proton path. The field reversed midway so that proton trajectories would be deviated negligibly. Our previous studies¹ used a magnetic spectrometer with emulsions for positive identification of ion species and momentum. Particle energy determined in that way agreed well with energy determined by time-of-flight measurement done simultaneously, using two collector screens to generate proton current wave forms. In the present work, the proton data were taken using the collector screens only. The first screen was 125 cm from the anode and 64.3 cm from the second collector. Reference 1 contains further details of the experimental arrangement.

Results

Data from each pulse consisted of eight or nine photographs of oscilloscope traces. Clearly it is impossible to present all of the details of these traces here. Instead, we have attempted to group the data into families of curves, extracting, to the best of our knowledge, the relevant part of the data for presentation. In this analysis, we have used the data only from the first pulse when multiple proton pulses were present.

Perhaps the most important data are summarized in figure 1a where observed proton energy is plotted as a function of hydrogen gas pressure for three cases. We tend to attribute the highest energy case (2 inch cathode, 1 MV beam) to the lowest temperature beam. This curve contains our highest observed proton energy (12.2 MeV) and has been previously reported.¹ The bell-shaped curve is especially interesting; unfortunately, Rogowski coil information is incomplete for these data. Figure 1b shows similar 1 inch cathode data (and one 3 inch cathode point) using a nominal 750 kV beam, but the scatter and inconsistency of these data are so great that we have chosen to concentrate on analysis of the 2 inch cathode 1 MV and 750 kV curves. The reasons for this scatter are unknown. Apparently, certain diode configurations and certain pressure regimes are stable while others are not.

Figure 2 shows the beam current front velocities for these two cases, measured between the 5 and 14.7 cm points, where β_b^2 is plotted versus pressure. The similarity between these curves and the proton energy curves is dramatic; this behavior has been noticed previously.^{1,2} Here we have defined the beam front as the leading edge of the current pulse, which in most cases is very sharply defined (sub-nsec) on the Rogowski coil wave forms. In all of our data, the proton bunch (typically 10 cm in length at the first collector) is always behind this leading edge, based on a linear proton trajectory extrapolation to the anode computed from observed proton arrival time and velocity in the diagnostic region. (Previously we confirmed that the proton bunch does have its origin quite near the anode.¹)

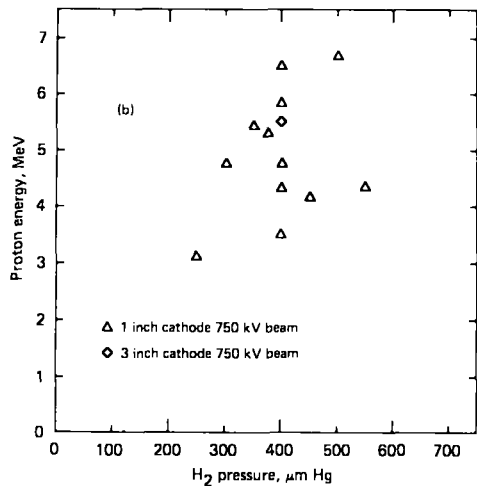
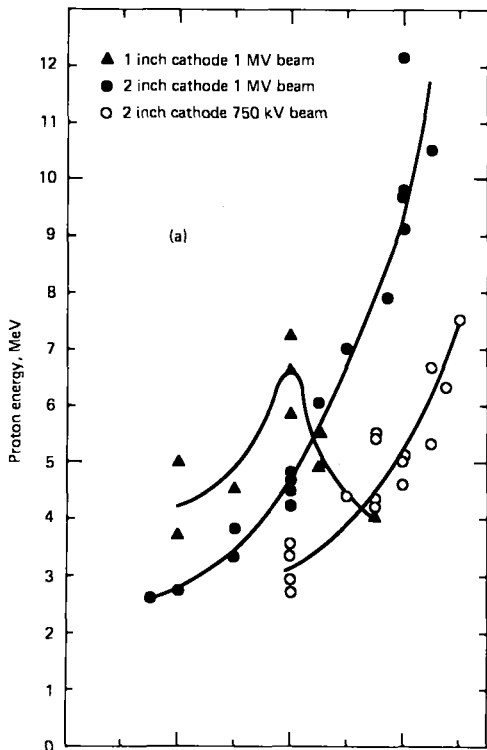


Figure 1 Proton energy versus hydrogen pressure, determined by time-of-flight of the peak amplitude of the proton waveform. Smooth curves are drawn through the data in this and subsequent figures.

We have computed a relative measure of total proton flux by integrating the proton current waveforms. These data, in figure 3, are given in most cases as pressure-bin averages because the individual values showed great fluctuation, occasionally by more than an order of magnitude at unchanged hydrogen pressure. Whether this reflects real variations in the total number of accelerated protons, or whether the spatial distribution of protons was off-axis and, as a result, not well sampled by our 1.1 cm aperture, is uncertain; the latter effect has been observed in other studies.³ The implication of figure 3 along with figure 1 is that the upper limit on the pressure regime for acceleration involves a dwindling particle flux.

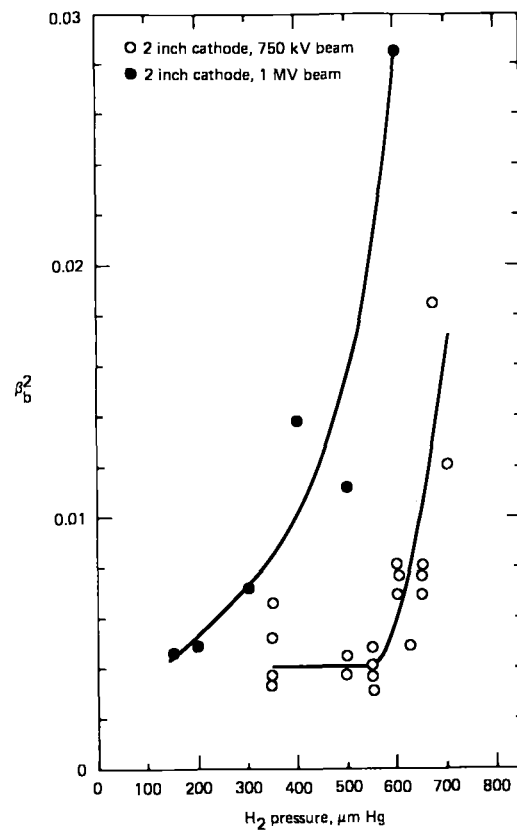


Figure 2 The square of the beam front velocity β_b versus hydrogen pressure. β_b was measured by the leading edge of Rogowski coils at 5 and 14.7 cm from the anode.

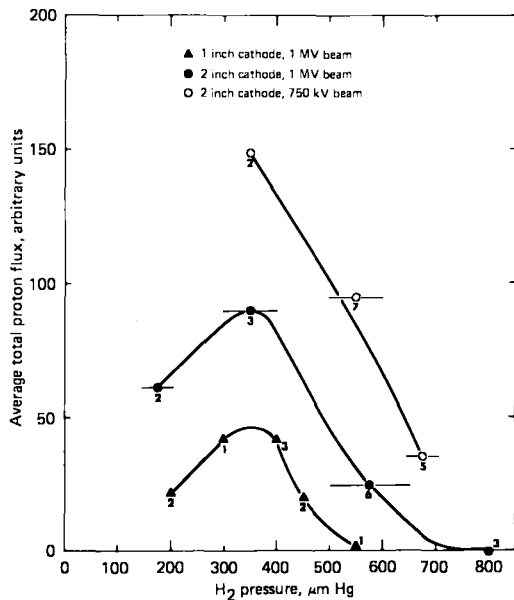


Figure 3 Average relative proton flux versus pressure, computed by integration of proton waveforms. Horizontal bar shows pressure bin in which the number of data points indicated, were averaged. The two 1 MV curves have the same absolute normalization.

The electron current in the acceleration tube has a well-defined rise time (typically 3 to 10 nsec), which we term the beam head. The extrapolated proton trajectories are always either within the beam head (most cases), or closely behind it. In view of this, we exhibit in figure 4 the calculated energy \mathcal{E}_0 given to a positive charge by the induced longitudinal electric field in the beam head, where dI/dt (typically 0.4 to 2.0×10^{13} A/sec) was measured versus distance by the four Rogowski coils. For protons the expression for \mathcal{E}_0 is

$$\mathcal{E}_0 \equiv \int eE_{\text{ind.}} dz = \frac{e\mu_0}{2\pi} \frac{dI}{dt} \left(1 + 2\ln \frac{r_w}{r_b}\right)$$

where e is the proton charge, r_w is the radius of the cylindrical chamber wall, and r_b is the radius of the beam (assumed to be uniform). We have set $r_b = r_w$ in computing \mathcal{E}_0 to account for radial expansion of the beam head due to incomplete charge neutralization. Note that the energy \mathcal{E}_0 would be transferred only if the protons were in step with the beam head along the entire length of the chamber. Of course, in experimentally selecting out and confining our study to pressures that gave the highest energies, we may have empirically chosen that parameter range where the protons are accidentally in step; or alternatively, a trapping or synchronizing mechanism may be operating. In either case, the correlation of higher proton energy with higher dI/dt is very apparent, as is the downturn in this calculated integral near those pressures where beam front velocity increases sharply and where proton acceleration cuts off. As a precautionary note, we point out that this calculation is sensitive to the exact interpretation of the beam current wave forms and may be too high by a factor of about two due to instrumental effects. The relative error seems smaller and is perhaps represented by the scatter of the points. We note that as a rule, dI/dt decreases away from the anode, in some cases by as much as a factor of four over the length of the chamber.

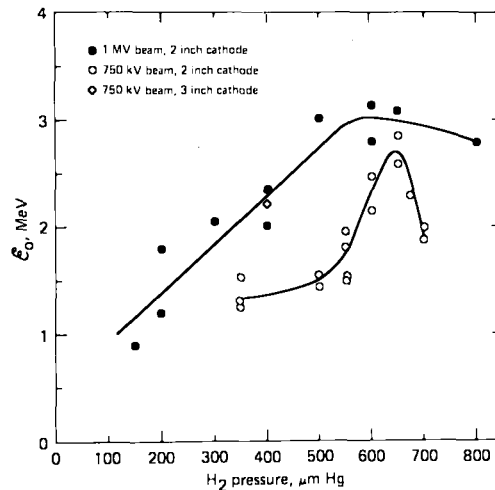


Figure 4 The energy gain \mathcal{E}_0 calculated from the induced electric field at the beam head versus pressure.

We have attempted to summarize important aspects of these data in the final two figures. Figure 5 is a correlation plot for all of our data of current front velocity versus proton velocity. General agreement is seen although the correlation is not precise. Of course, since in most cases the beam current front is mildly accelerating once it leaves the anode region, this comparison of proton velocity with beam velocity at one part of its trajectory could not be expected to be complete. Figure 6 shows the correlation plot of "inductive" energy versus observed particle energy for all of our data. A correlation is seen, as is the fact that the inductive energy contributes only a part of the final proton energy. We know that fields of at least 300 kV/cm exist near the anode (see ref. 1 where at least 3 MeV protons were seen to come from the region within 10 cm from the anode). This seems to be at least three to six times larger than the strongest fields induced by dI/dt observed in the anode vicinity. We interpret these data as indicating that the observed acceleration is due to both induced and space charge fields, and that the latter (i.e., electrostatic) field of order 10^6 V/cm predominates near the anode.

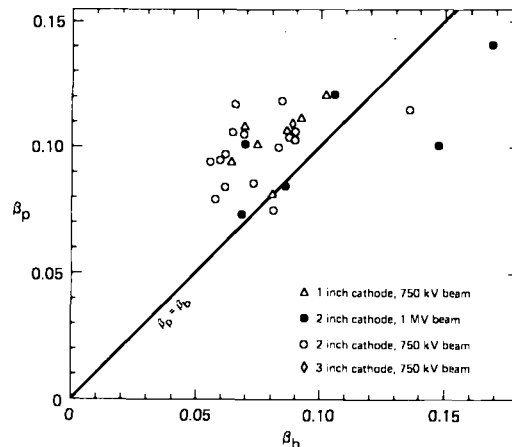


Figure 5 Proton and beam front velocity correlation plot.

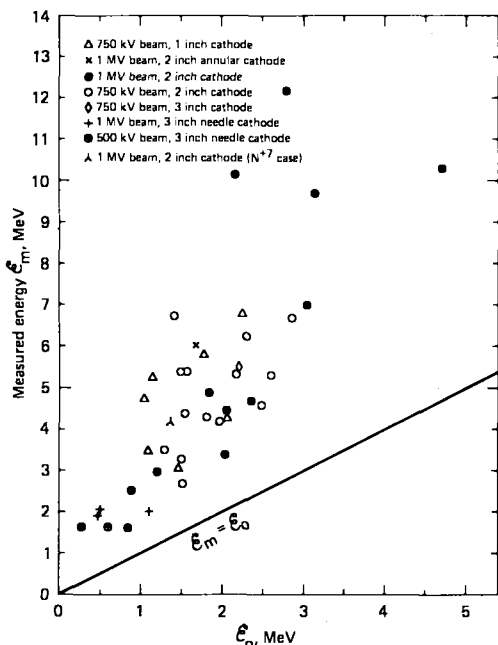


Figure 6 Correlation plot of measured particle energy E_m and calculated energy E_0 . Data refer to accelerated protons in all cases except the point marked λ , which refers to 29 MeV N^{+7} ions. For this case, energies are MeV/Z.

Conclusions

Our experimental results, new and previously reported (marked below by an asterisk*), can be summarized as the following tentative conclusions:

1. Agreement between the beam current front velocity and proton velocity exists. (See also reference 1 and 2.)
2. Part of the proton energy apparently is generated by the induced medium strength electric field in the beam head over the length of the beam propagation chamber.
- 3.* There is evidence that a high field, short-distance launch occurs near the anode: at least 300 kV/cm, perhaps 1 MV/cm, over 10 cm.¹
- 4.* The proton bunch has a small longitudinal extent, typically 10 cm after moving more than a meter, and is associated with the beam head, consistent with the idea of a high-field launch near the anode.^{1,6}
- 5.* Weak longitudinal magnetic fields (≈ 500 G) drastically reduce proton flux without affecting proton energy.¹
6. An upper limit pressure region exists, near 600 to 700 microns in hydrogen for our 2-inch beams, where
 - a) beam front velocity increases dramatically,
 - b) proton energies are highest but proton flux decreases severely, perhaps to zero.
- 7.* Ion energies are Z times proton energies, where Z is observed ionic charge.^{1,6}
- 8.* Multiple pulses are observed under certain appropriate beam and pressure conditions.^{5,6}
- 9.* The number of accelerated protons per beam pulse is 10^{12} to 10^{13} , and protons up to 12.2 MeV and N^{+7} ions at 29 MeV have been observed.¹

With the detection of coherent electrostatic accelerating fields of order 10^6 V/cm, the usefulness of the technique depends upon the extension of the acceleration length, which in our work was of order 10 cm. How this can be done depends upon the physics of the electron charge cloud that causes the field. The space charge structure may be produced by primarily longitudinal effects,⁷ and/or radial effects may be involved.⁸ Our observation¹ that weak longitudinal magnetic fields (~ 500 gauss) severely affected the acceleration process means that two-dimensional effects must be involved.

The observed velocity agreement between beam front and proton bunch and the fact that beam front velocities of up to $\beta_D = 0.7$ have been observed in hydrogen at uniform pressure⁹ indicate that a way to take advantage of the increasing beam velocity with increasing pressure may be to use a pressure gradient in the acceleration tube. This would avoid the proton flux cut-off by starting acceleration at a pressure that gives high flux, and then proceeding continuously to higher pressures where beam front and bunch velocity increase.

Kuswa¹⁰ and Swain, Kuswa, Poukey and Olson¹¹ have performed pressure gradient experiments along these lines, and did not detect increased proton energy. However, they had significantly slower electron beam risetime than used in the present studies, and according to the theory of Olson,¹² this would mitigate the effect of the gradient.³ The very broad proton pulses of Swain et al. is further indication that their study and ours have treated significantly different parameter regimes.

The observation of multiple ion bunches (2 to 4 bunches arriving at the collector screens up to 60 nsec apart) may have significant implications about the acceleration and charge production processes. If, for example, these bunches are associated with time-separated space charge fields, then space charge neutralization cannot be complete behind the first bunch or, indeed, behind the risetime portion of the beam.

We conclude with a discussion of energy balance. Since the bunch velocity appears limited by the beam front velocity, we examine the energetic constraints on beam front velocity. The beam power injected from the diode is $P_d = I_d V$, where I_d is diode current and V is diode voltage. This power, which represents purely beam kinetic energy at the anode plane, is distributed during beam propagation into plasma energy (ionization, the driving of plasma currents, and plasma heating), the kinetic energy of an accelerated proton or ion bunch, electromagnetic waves (e.g., microwaves), electric fields, and magnetic fields. Here we treat only the last of these, which with our parameters turns out to imply by itself a velocity limitation.

Consider a simple model in which the beam front has reached its final propagation velocity β_{bc} . This velocity is less than the electron longitudinal streaming velocity $\beta_{||} c$, which in turn is less than the total electron velocity β_{ec} . The distance from anode to beam front is $l = \beta_{bc} ct$. For simplicity, we assume a sharp beam front. Ignoring end effects, the conversion rate of beam kinetic energy into magnetic field energy is

$$P_m = \frac{\partial}{\partial t} \int \frac{B^2}{2\mu_0} d^3x = \frac{\partial}{\partial t} \frac{1}{2} LI_n^2,$$

where L is the inductance of beam propagation and I_n is the net beam current. Explicitly,

$$P_m = \frac{\partial}{\partial t} k \dot{I}_n^2 = k (\dot{I}_n \dot{I}_n + I_n^2 \dot{l}),$$

where $k \equiv (\mu_0/4\pi) [1 + 2\ln(r_w/r_b)]$ and a dot ($\dot{}$) signifies $\partial/\partial t$. With $l = \beta_{bc} ct$, energy conservation (neglecting all the other possible losses) requires

$$\frac{P_m}{P_d} = \frac{k (\dot{I}_n \dot{I}_n + \beta_{bc} I_n^2 \dot{l})}{I_d V} < 1 \quad (1)$$

assuming that injected beam energy is not stored over time and then quickly converted to magnetic field energy by some unknown process. We choose the time $t = 7$ nsec to evaluate the above ratio, because Rogowski coil data shows that typically the beam front has by this time accelerated away from the anode and attained a "final" velocity that increases slowly thereafter, if at all. Then $l \approx 0.2$ m, $I_n \approx 65$ kA, $\dot{I}_n \approx 10^{13}$ A/sec, $\beta_b \approx 0.09$, $I_d \approx 70$ kA, $k = 10^{-7}$ henry/m and $V \approx 6 \times 10^5$ volts. These figures give $P_m/P_d = 0.58$. In addition it is to be noted that the energy for P_m comes from the beam's longitudinal kinetic energy, which with $v/\gamma = 2$ must be assumed to be substantially less than the total kinetic energy.¹³ It therefore appears very probable that in our study the beam front (and proton bunch) velocity was limited by power input. This effect has also been deduced in other studies.^{1,14} If true, this is a promising result because P_m is quite sensitive to I_n ; for example, decreasing I_d (and therefore I_n and \dot{I}_n) by a factor of 2, and increasing V by the same factor, allows an increase of β_b by a factor of 8 in equation (1) without increasing the ratio P_m/P_d . These effects may explain why in figure 1 the 1 MV, 2 inch beam gave higher proton energies than the 750 kV, 2 inch beam, and why in figure 2 the beam front velocity increases so sensitively with pressure. The clear implication of the energetic constraints is that beam voltage and current profiles must be properly tailored to achieve higher particle energies.

References

1. B. Ecker, S. Putnam, D. Drickey, IEEE Trans. Nuc. Sci. NS-20, Series 3, 301 (1973).
2. J. Rander, Phys. Rev. Letters, 25, 893 (1970).
3. G. Kuswa, Sandia Laboratories (private communication).
4. S. Putnam, Phys. Rev. Letters 25, 1129 (1970).
5. S. Putnam, IEEE Trans. Nuc. Sci. NS-18, 496 (1971).
6. J. Rander, B. Ecker, G. Yonas and D. Drickey, Phys. Rev. Letters 24, 283 (1970).
7. N. Rostoker, "Acceleration of Ions in Intense MeV Electron Beams," VII International Conference on High Energy Acceleration, Yerevan, Armenia, USSR (1969); S. Graybill, et al., DASA Report No. 2477, Defense Nuclear Agency, Washington, D.C. (1970).
8. Radial electrostatic effects include both the mechanism of localized pinch model (references 4 and 5) and radial blowup in the beam head due to beam space charge forces.
9. J. Rander et al., Physics International Company Report No. PIIR-2-71 (unpublished).
10. G. Kuswa, Annals of the New York Academy of Science, 1974 (to be published).
11. D. Swain, G. Kuswa, J. Poukey and C. Olson, to be published in the Proceedings of the IXth International Conference on High Energy Accelerators, Stanford, California, May 1974.
12. C. Olson, to be published in the Proceedings of the IXth International Conference on High Energy Accelerators, Stanford, California, May 1974.
13. The observed net currents in our studies were typically 84 kA, which is twice the Alfvén limiting current, so $(v/\gamma)_{net} = 2$. Radial electrostatic fields can relax the Alfvén current limitation, and this observation may be evidence of the existence of such fields over substantial portions of the beam pulse width.
14. G. Yonas, P. Spence, B. Ecker, Current Neutralization in High v/γ Relativistic Electron Streams, Physics International Company Report No. PIIR-8-70 (1969).